Journal of Sound and Vibration (2002) **258**(1), 95–122
doi:10.1006/jsvi.5073, available online at http://www.idealibrary.com on IDEAL®

ON THE FALSE DEGENERACY OF THE HELMHOLTZ BOUNDARY INTEGRAL EQUATIONS

W. Yeih, S. R. Kuo and R. F. Liu

Department of Harbor and River Engineering, National Taiwan Ocean University, 2 Pei-Ning Road, Keelung, Taiwan 202, Republic of China. E-mail: wcyeih@mlab.hre.ntou.edu.tw

AND

J. R. Chang

Department of System Engineering and Naval Architecture, National Taiwan Ocean University, 2 Pei-Ning Road, Keelung, Taiwan 202, Republic of China

(*Received 2 October* 2001, *and in final form 7 February* 2002)

In this paper, the false degeneracy of the Helmholtz boundary integral equations is examined. A new theory to explain the false degeneracy of the Helmholtz boundary integral equations is given. In this proposed theory, a false degeneracy of the boundary integral equation is explained as finding a non-trivial source distribution such that it results in trivial field quantities inside the domain interested and non-trivial field quantities for its counter part, i.e., outside the domain interested. It is clearly explained that such a false degeneracy is independent of prescribed boundary conditions but dependent on the integral equation one selects. Moreover, the false degeneracy of the integral equation for the interested domain relates to the eigenproblem for its counter part. Under such a unified theory, the fictitious eigenvalue, spurious eigenvalue and pseudo-fictitious eigenvalue can be explained in a simple mathematical frame. It is concluded from our theoretical analysis that a multiply connected domain results in the pseudo-fictitious eigenvalue even the complex-valued formulations are used. In order to eliminate various kinds of false degeneracy, two methods are employed according to the previous research. A unified view of these two methods is provided such that they can be thought to be equivalent from mathematical point of view. Several numerical examples are given to show the validity of current approach.

1. INTRODUCTION

The eigenproblem is very important in engineering. For design engineers, the natural frequencies of a structure system is essentially important since a catastrophic failure would happen once the frequency of the driving force coincides with these natural frequencies. Further, the mode superposition method is based on the analysis of an eigenproblem, which is a well-known result of the Fredholm theory of the linear operator. Therefore, the eigenproblem may be viewed as the first step to tackle the vibration problem.

Because of the complexity, some engineering problems ought to be solved by numerical methods, e.g., the finite element method, the finite difference method and the boundary element method. For treating the eigenproblem in the boundary element method, the complex-valued formulation is required theoretically [1, 2]. In order not to deal with the complicate computation in complex-valued formulation, a simplified method using the real-part formulation or imaginary-part formulation has been proposed by De Mey [3]. However, this simplified method will result in some side effects such as spurious eigensolutions [4], and numerical instability in the imaginary-part formulation [5]. The spurious eigenvalues can be easily detected by the set of dual boundary integral equations since they cannot satisfy both equations (singular and hypersingular integral equations) at the same time and thus must not be true eigenvalues. This idea was first proposed to filter out the spurious eigenvalues by Chen and Wong [6]. It was later extended [7, 8] using the singular value decomposition method to check the rank of an overdetermined system constructed by the real-part singular and hypersingular integral equations together. Another approach to eliminate spurious eigenvalues comes from the work of Chang *et al.* [9]. In this work, they showed that the spurious eigenvalue could be detected within the singular integral equation or hypersingular integral equation alone by simply moving the artificial boundary of the domain partitioning, i.e., extra information from the counter part of dual integral formulation is not necessary. Later, Kuo *et al.* [5] proposed a deep insight of this new approach. They have explained that the occurrence of spurious eigenvalues is due to the simultaneous rank deficiencies of the influence matrices that appear at the right-hand side and left-hand side of the equations constructed by the incomplete BEM. It means that an indefinite form of 0/0 is encountered in this formulation. Besides, Kuo *et al.* also gave an explanation and the solution technique for the ill-posed behavior of a regular formulation, i.e., the formulation without any singular integrals and hypersingular integrals. The regular formulation is not our major concern and a review of the literature relating to this topic can be found in reference [5].

The main goal of this research is to solve the eigenproblem by various singular-type direct BEM formulations with the domain partitioning technique as the beginning. The reason why we concern this kind of problem is given as follows. For solving a spatially distributed loading case, the domain partition becomes necessary in order to separate the domain into a loaded zone and an unloaded one [10]. Moreover, a domain partition technique is also necessary for a domain composed by several different materials. After domain partitioning, one can solve the integral equations resulting from each subdomain and the interface transmission conditions together. As shown in our previous work [9], one can expect that the spurious eigenvalues for the real-part formulation may occur at different values when the partitioning position moves. We will demonstrate this in one of our numerical examples. Furthermore, when the domain partition is adopted it is possible for us to have a subdomain that is a multiply connected region in nature. For such a multiply connected subdomain, we find numerically and analytically that a new type of spurious eigenvalues exists no matter a real-part or a complex-valued formulation is adopted. The main contribution of this research is in a higher level than solving an eigenproblem with domain partitioning. We try to unify all phenomena of the false degeneracy for the Helmholtz boundary integral equation in a single mathematical frame.

In what followings, section 2 describes the theoretical background on the dual direct BEM formulation under the condition of domain partitioning for the free vibration problem. In addition, the methods to filter out the spurious eigenvalue are briefly reviewed. Moreover, several analytical derivations of true or spurious eigenvalues for different designed numerical examples are also included here. To unify all kinds of the false degeneracy, a mathematical theory is given in section 3. Under such a theory, several facts can be yielded simply. In section 4, numerical examples are employed to validate the analytical prediction. At the same time, some interesting discoveries explored on the numerical and analytical results will also be addressed here. Finally, we close with some important conclusions by recasting the current research in section 5.

2. THEORETICAL BACKGROUND AND DERIVATIONS

2.1. DUAL INTEGRAL FORMULATIONS FOR A TWO-DIMENSIONAL VIBRATION PROBLEM OF A MEMBRANE

Considering a free vibration problem for a 2-D membrane, the governing equation is

$$(\nabla^2 + k^2)u(\mathbf{x}) = 0, \quad \mathbf{x} \in \Omega \tag{1}$$

where $u(\mathbf{x})$ represents the displacement at point $\mathbf{x}$, ∇^2 is the Laplacian operator, Ω is the domain considered and k is the wave number which is the frequency over the wave speed. Based on the complex-valued dual formulations, the dual integral equations for the direct-BEM can be derived [11]:

(direct, singular integral equation: UT equation)

$$cu(\mathbf{s}) = RPV \int_{\Gamma} U_C(\mathbf{x},\mathbf{s})t(\mathbf{x})\,\mathrm{d}\Gamma(\mathbf{x}) - CPV \int_{\Gamma} T_C(\mathbf{x},\mathbf{s})u(\mathbf{x})\,\mathrm{d}\Gamma(\mathbf{x}), \tag{2}$$

(direct, hypersingular integral equation: LM equation)

$$ct(\mathbf{s}) = CPV \int_{\Gamma} L_C(\mathbf{x},\mathbf{s})t(\mathbf{x})\,\mathrm{d}\Gamma(\mathbf{x}) - HPV \int_{\Gamma} M_C(\mathbf{x},\mathbf{s})u(\mathbf{x})\,\mathrm{d}\Gamma(\mathbf{x}), \tag{3}$$

where CPV, RPV and HPV denote the Cauchy principal value, the Riemann principal value and the Hadamard principal value respectively; $t(\mathbf{s}) \equiv \partial u(s)/\partial n_s$ with n_s denotes the outnormal direction at point $\mathbf{s}$; Γ denotes the boundary enclosing Ω. It should be noted that when $\mathbf{s} \in \Omega$, the constant, c, is equal to 2π; while $\mathbf{s} \in \Gamma$ and $\mathbf{s} \notin \Omega$, c is equal to π on the smooth boundary. The four kernels are complex with the following properties: $(\nabla^2 + k^2)U_C(\mathbf{x},\mathbf{s}) = 2\pi\delta(\mathbf{x} - \mathbf{s})$ and $U_C(\mathbf{x},\mathbf{s})$ satisfies the radiation condition, $T_C(\mathbf{x},\mathbf{s}) \equiv \partial U_C(\mathbf{x},\mathbf{s})/\partial n_{\mathbf{s}}$, $L_C(\mathbf{x},\mathbf{s}) \equiv \partial U_C(\mathbf{x},\mathbf{s})/\partial n_{\mathbf{x}}$ and $M_C(\mathbf{x},\mathbf{s}) \equiv \partial^2 U_C(\mathbf{x},\mathbf{s})/\partial n_{\mathbf{s}}\partial n_{\mathbf{x}}$. As well known, the real-part BEM has been adopted to avoid the complex-valued calculations for the computational efficiency. The four real-part kernels of the complex-valued ones are defined as

$$U_R(\mathbf{x},\mathbf{s}) \equiv \mathrm{Real}(U_C(\mathbf{x},\mathbf{s})), \quad T_R(\mathbf{x},\mathbf{s}) \equiv \mathrm{Real}(T_C(\mathbf{x},\mathbf{s})),$$

$$L_R(\mathbf{x},\mathbf{s}) \equiv \mathrm{Real}(L_C(\mathbf{x},\mathbf{s})), \quad M_R(\mathbf{x},\mathbf{s}) \equiv \mathrm{Real}(M_C(\mathbf{x},\mathbf{s})).$$

Details of various boundary integral formulations of direct type can be referred in reference [5]. Since we will adopt domain partitioning in the following numerical examples, a brief introduction of constructing integral equations in such a scheme is given as follows. Consider the domain is partitioned as shown in Figure 1, after performing a finite discretization in each subdomain, equations (2) and (3) can be symbolically written as a set of linear algebraic equations with the boundary and interface conditions in the following:

(direct, singular integral equation: UT equation)

$$\begin{bmatrix} \overline{\mathbf{T}}_{rr} & \overline{\mathbf{T}}_{ri} & \mathbf{U}_{rr} & \mathbf{U}_{ri} \\ \overline{\mathbf{T}}_{ir} & \overline{\mathbf{T}}_{ii} & \mathbf{U}_{ir} & \mathbf{U}_{ii} \\ \mathbf{l}_r & \mathbf{0} & \mathbf{m}_r & \mathbf{0} \\ \mathbf{0} & \mathbf{c}_i & \mathbf{0} & \mathbf{0} \\ \mathbf{0} & \mathbf{0} & \mathbf{0} & \mathbf{d}_i \end{bmatrix} \begin{bmatrix} \mathbf{u}_r \\ \mathbf{u}_i \\ \mathbf{t}_r \\ \mathbf{t}_i \end{bmatrix} = \begin{bmatrix} \mathbf{0} \\ \mathbf{0} \\ \mathbf{0} \\ \mathbf{0} \\ \mathbf{0} \end{bmatrix}, \tag{4}$$

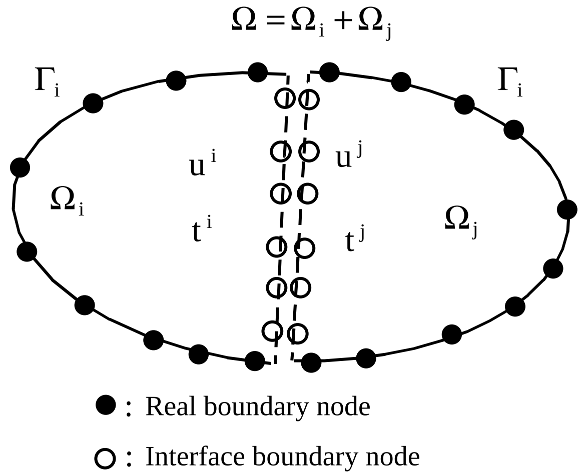

Figure 1. An illustrative idea of domain partitioning.

(direct, hypersingular integral equation: LM equation)

$$\begin{bmatrix} \mathbf{M}_{rr} & \mathbf{M}_{ri} & \overline{\mathbf{L}}_{rr} & \overline{\mathbf{L}}_{ri} \\ \mathbf{M}_{ir} & \mathbf{M}_{ii} & \overline{\mathbf{L}}_{ir} & \overline{\mathbf{L}}_{ii} \\ \mathbf{l}_r & \mathbf{0} & \mathbf{m}_r & \mathbf{0} \\ \mathbf{0} & \mathbf{c}_i & \mathbf{0} & \mathbf{0} \\ \mathbf{0} & \mathbf{0} & \mathbf{0} & \mathbf{d}_i \end{bmatrix} \begin{bmatrix} \mathbf{u}_r \\ \mathbf{u}_i \\ \mathbf{t}_r \\ \mathbf{t}_i \end{bmatrix} = \begin{bmatrix} \mathbf{0} \\ \mathbf{0} \\ \mathbf{0} \\ \mathbf{0} \\ \mathbf{0} \end{bmatrix}, \tag{5}$$

where the subscript r denotes the collocation on the real boundary, subscript i denotes the collocation on the interfaces between subdomains; $\mathbf{l}_r\mathbf{u}_r + \mathbf{m}_r\mathbf{t}_r = 0$ represents the boundary condition given on the real boundary; $\mathbf{c}_i\mathbf{u}_i = 0$ and $\mathbf{d}_i\mathbf{t}_i = 0$ represent the interface transmission conditions.

It should be noted that in equations (4) and (5), either the complex-valued or real-valued kernels can be used and these equations actually combine all the information including the described boundary integral equations, boundary conditions and interface conditions together in a matrix form. We refer to such an approach subsequently as the conventional approach.

2.2. TECHNIQUES OF ELIMINATING SPURIOUS EIGENVALUES

The real-part formulation will result in spurious eigenvalues. Yeih *et al.* [12] explained the reason of spurious eigenvalues as lacking information contributed by the imaginary part kernel. To filter out spurious eigenvalues, two methodologies have been proposed and will be briefly reviewed in the followings.

The first method simply tries to compensate the insufficient information by providing further information from the framework of dual integral equations. It means to construct an overdetermined system using both real-part equations (singular and hypersingular) and the rank deficiency occurring at the spurious eigenvalue can be avoided due to additional information [7, 8].

Another approach comes from a different point of view [5]. Considering that not to use another equation from the dual integral equations, can one give additional information? Kuo *et al.* [5] proposed that one could construct an auxiliary boundary value problem with linearly independent boundary conditions. These two problems can be combined together to pick out the spurious eigenvalues since they proved that for these two problems the spurious eigensolutions must be the same.

Although the above-mentioned two methods look different, they can be related as in the following. Remember that for the second method, 0/0 form is encountered. Analytically speaking, the value can only be determined by performing the L'Hospital rule, which means to give the information form the derivative of original functions. Let us look back to the first approach, the hypersingular integral equation happens to be the normal derivative of the singular integral equation. Therefore, they can compensate each other to perform L'Hospital rule due to the sufficient information.

2.3. ANALYTICAL STUDY FOR RANK DEFICIENCIES

In the following, we will employ the properties of the circulant and degenerated kernel to derive the rank deficiencies, either true eigenvalues or spurious ones, of influencing matrices for several cases. The detailed derivation can be found in references [5, 13]. Now considering that a source, **s**, is located on a circular boundary with radius R and a collocation point, **x**, is located on another circular boundary with radius $\bar{r}$. These two circles have a common center, says O that is defined as the origin. The angle between position vectors of **x** and **s** is defined as θ and the distance between these two points is defined as ρ. The setup of above-mentioned notations is shown in Figure 2. Then from the properties of the degenerated kernel, one has

$$\mathrm{Y}_0(k\rho) = \mathrm{Y}_0(k\sqrt{R^2 + \bar{r}^2 - 2R\bar{r}\cos\theta}) = \begin{cases} \sum_{m=-\infty}^{\infty} \mathrm{Y}_m(kR)\mathrm{J}_m(k\bar{r})\cos(m\theta) & \text{for } R > \bar{r}, \\ \sum_{m=-\infty}^{\infty} \mathrm{J}_m(kR)\mathrm{Y}_m(k\bar{r})\cos(m\theta) & \text{for } \bar{r} > R \end{cases} \tag{6}$$

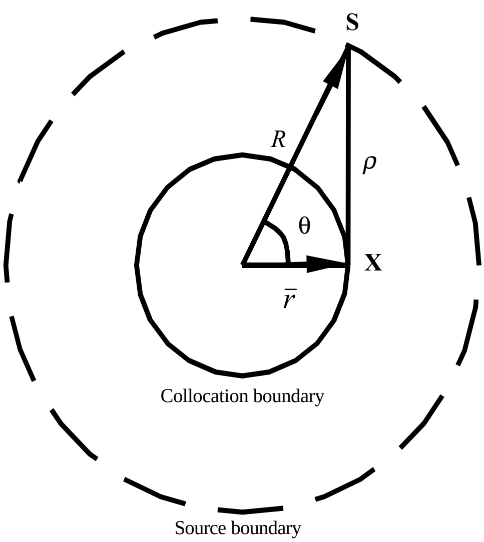

Figure 2. An illustration of source points and collocation points.

and

$$\mathrm{J}_0(k\rho) = \mathrm{J}_0\left(k\sqrt{R^2 + \bar{r}^2 - 2R\bar{r}\cos\theta}\right) = \sum_{m=-\infty}^{\infty} \mathrm{J}_m(kR)\mathrm{J}_m(k\bar{r})\cos(m\theta) \tag{7}$$

Without lengthy derivation, results are shown directly in Tables 1–3.

In Table 2, we try to analyze the eigenproblem of a circular domain by partitioning it into two subdomains: a circle with a radius r_2 and an annular region with an inner radius r_2 and an outer radius r_1. It can be found in Table 2 that a new type of spurious eigenvalue occurs when a complex-valued formulation is used. Chang [14] named this type as the pseudo-fictitious eigenvalue. Chang pointed out that this pseudo-fictitious eigenvalue occurs due to the geometry of a multiply connected domain. He showed analytically by using an annular region with an inner radius r_2 and an outer radius r_1 giving different boundary conditions. These results are shown in Table 3. It can be found that the pseudo-fictitious eigenvalue occurs again no matter which kind of boundary conditions is prescribed in this problem.

From these two tables, one can find two interesting things: first, the false rank deficiency, no matter whether due to the spurious eigenvalue or pseudo-fictitious eigenvalue, is independent of boundary condition but dependent on which integral equation one uses; second, once the integral equation is chosen the pseudo-fictitious

TABLE 1

Characteristics of eigenequations for a circular domain by using various dual BEM formulations

	True eigenequation	Spurious eigenequation
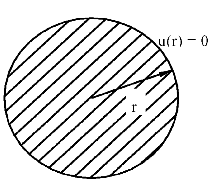		
Dirichlet case		
Complex UT formulation	$\mathrm{J}_m(kr) = 0$	—
Complex LM formulation	$\mathrm{J}_m(kr) = 0$	—
Real-part UT formulation	$\mathrm{J}_m(kr) = 0$	$\mathrm{Y}_m(kr) = 0$
Real-part LM formulation	$\mathrm{J}_m(kr) = 0$	$\mathrm{Y}'_m(kr) = 0$
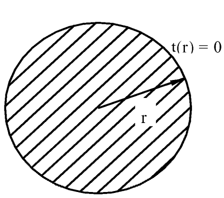		
Neumann case		
Complex UT formulation	$\mathrm{J}'_m(kr) = 0$	—
Complex LM formulation	$\mathrm{J}'_m(kr) = 0$	—
Real-part UT formulation	$\mathrm{J}'_m(kr) = 0$	$\mathrm{Y}_m(kr) = 0$
Real-part LM formulation	$\mathrm{J}'_m(kr) = 0$	$\mathrm{Y}'_m(kr) = 0$

TABLE 2

Characteristics of eigenequations for a partitioned circular subdomain and an annular circular one by using various dual BEM formulations

	True eigenequation	Pseudo-fictitious eigenequation	Spurious eigenequation
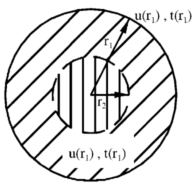 Boundary condition : u(r1) = 0			
Dirichlet case			
Complex UT formulation	$J_m(kr_1) = 0$	$J_m(kr_2) = 0$	—
Complex LM formulation	$J_m(kr_1) = 0$	$J'_m(kr_2) = 0$	—
Real-part UT formulation	$J_m(kr_1) = 0$	$J_m(kr_2) = 0$	$Y_m(kr_1) = 0$ and $Y_m(kr_2) = 0$
Real-part LM formulation	$J_m(kr_1) = 0$	$J'_m(kr_2) = 0$	$Y'_m(kr_1) = 0$ and $Y'_m(kr_2) = 0$
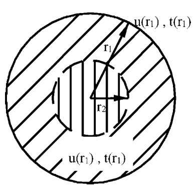 Boundary condition : t(r1) = 0			
Neumann case			
Complex UT formulation	$J'_m(kr_1) = 0$	$J_m(kr_2) = 0$	—
Complex LM formulation	$J'_m(kr_1) = 0$	$J'_m(kr_2) = 0$	—
Real-part UT formulation	$J'_m(kr_1) = 0$	$J_m(kr_2) = 0$	$Y_m(kr_1) = 0$ and $Y_m(kr_2) = 0$
Real-part LM formulation	$J'_m(kr_1) = 0$	$J'_m(kr_2) = 0$	$Y'_m(kr_1) = 0$ and $Y'_m(kr_2) = 0$

eigenvalue depends on the geometry of inner hole only. However, in Chang's dissertation the general proofs for these two findings were not provided.

3. A GENERAL THEORY FOR THE FALSE DEGENERACY OF BOUNDARY INTEGRAL EQUATIONS

3.1. FALSE DEGENERACY IN INDIRECT BEM

Before we provide our new point of view, we first review the integral equations from another aspect: the indirect BEM. The indirect BEM represents the field quantities by superposition of the influence of the single-layer potential or a double-layer potential. It can be written as

(indirect method: single-layer potential)

$$\pi u(\mathbf{x}) = \int_\Gamma U_C(\mathbf{x}, \mathbf{s})\phi(\mathbf{s})\,\mathrm{d}\Gamma(\mathbf{s}), \tag{8a}$$

$$\pi t(\mathbf{x}) = \int_\Gamma \frac{\partial U_C(\mathbf{x}, \mathbf{s})}{\partial n_\mathbf{x}}\phi(\mathbf{s})\,\mathrm{d}\Gamma(\mathbf{s}) = \int_\Gamma L_C(\mathbf{x}, \mathbf{s})\phi(\mathbf{s})\,\mathrm{d}\Gamma(\mathbf{s}) \tag{8b}$$

TABLE 3

Characteristics of eigenequations for an annular circular domain by using various dual BEM formulations

	True eigenequation	Pseudo-fictitious eigenequation	Spurious eigen-equation
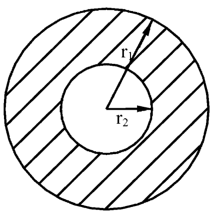			
Boundary condition : $u(r_1) = 0$; $u(r_2) = 0$			
Dirichlet case			
Complex UT formulation	$J_m(kr_2)Y_m(kr_1) - J_m(kr_1)Y_m(kr_2) = 0$	$J_m(kr_2) = 0$	—
Complex LM formulation	$J_m(kr_2)Y_m(kr_1) - J_m(kr_1)Y_m(kr_2) = 0$	$J'_m(kr_2) = 0$	—
Real-part UT formulation	$J_m(kr_2)Y_m(kr_1) - J_m(kr_1)Y_m(kr_2) = 0$	$J_m(kr_2) = 0$	$Y_m(kr_1) = 0$
Real-part LM formulation	$J_m(kr_2)Y_m(kr_1) - J_m(kr_1)Y_m(kr_2) = 0$	$J'_m(kr_2) = 0$	$Y'_m(kr_1) = 0$
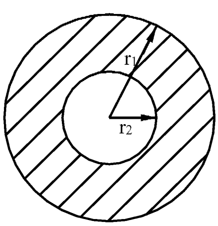			
Boundary condition : $t(r_1) = 0$; $t(r_2) = 0$			
Neumann case			
Complex UT formulation	$J'_m(kr_2)Y'_m(kr_1) - J'_m(kr_1)Y'_m(kr_2) = 0$	$J_m(kr_2) = 0$	—
Complex LM formulation	$J'_m(kr_2)Y'_m(kr_1) - J'_m(kr_1)Y'_m(kr_2) = 0$	$J'_m(kr_2) = 0$	—
Real-part UT formulation	$J'_m(kr_2)Y'_m(kr_1) - J'_m(kr_1)Y'_m(kr_2) = 0$	$J_m(kr_2) = 0$	$Y_m(kr_1) = 0$
Real-part LM formulation	$J'_m(kr_2)Y'_m(kr_1) - J'_m(kr_1)Y'_m(kr_2) = 0$	$J'_m(kr_2) = 0$	$Y'_m(kr_1) = 0$
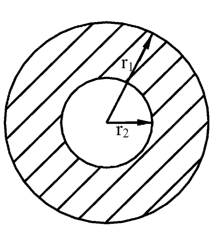			
Boundary condition : $u(r_1) = 0$; $t(r_2) = 0$			
Outer radius: Dirichlet Inner radius: Neumann			
Complex UT formulation	$J'_m(kr_2)Y_m(kr_1) - J_m(kr_1)Y'_m(kr_2) = 0$	$J_m(kr_2) = 0$	—
Complex LM formulation	$J'_m(kr_2)Y_m(kr_1) - J_m(kr_1)Y'_m(kr_2) = 0$	$J'_m(kr_2) = 0$	—
Real-part UT formulation	$J'_m(kr_2)Y_m(kr_1) - J_m(kr_1)Y'_m(kr_2) = 0$	$J_m(kr_2) = 0$	$Y_m(kr_1) = 0$
Real-part LM formulation	$J'_m(kr_2)Y_m(kr_1) - J_m(kr_1)Y'_m(kr_2) = 0$	$J'_m(kr_2) = 0$	$Y'_m(kr_1) = 0$

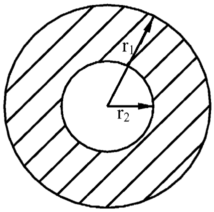

Boundary condition : $t(r_1) = 0$; $u(r_2) = 0$

Outer radius: Neumann
Inner radius: Dirichlet

Complex UT formulation	$J_m(kr_2)Y'_m(kr_1) - J'_m(kr_1)Y_m(kr_2) = 0$	$J_m(kr_2) = 0$	—
Complex LM formulation	$J_m(kr_2)Y'_m(kr_1) - J'_m(kr_1)Y_m(kr_2) = 0$	$J'_m(kr_2) = 0$	—
Real-part UT formulation	$J_m(kr_2)Y'_m(kr_1) - J'_m(kr_1)Y_m(kr_2) = 0$	$J_m(kr_2) = 0$	$Y_m(kr_1) = 0$
Real-part LM formulation	$J_m(kr_2)Y'_m(kr_1) - J'_m(kr_1)Y_m(kr_2) = 0$	$J'_m(kr_2) = 0$	$Y'_m(kr_1) = 0$

and

(indirect method: double-layer potential)

$$\pi u(\mathbf{x}) = \int_\Gamma \frac{\partial U_C(\mathbf{x},\mathbf{s})}{\partial n_\mathbf{s}} \psi(\mathbf{s})\, \mathrm{d}\Gamma(\mathbf{s}) = \int_\Gamma T_C(\mathbf{x},\mathbf{s})\psi(\mathbf{s})\, \mathrm{d}\Gamma(\mathbf{s}), \tag{9a}$$

$$\pi t(\mathbf{x}) = \int_\Gamma \frac{\partial^2 U_C(\mathbf{x},\mathbf{s})}{\partial n_\mathbf{x} \partial n_\mathbf{s}} \psi(\mathbf{s})\, \mathrm{d}\Gamma(\mathbf{s}) = \int_\Gamma M_C(\mathbf{x},\mathbf{s})\psi(\mathbf{s})\, \mathrm{d}\Gamma(\mathbf{s}), \tag{9b}$$

where Γ is a closed boundary, $\phi(\mathbf{s})$ is the single-layer potential density function and $\psi(\mathbf{s})$ is the double-layer potential density function. From the equivalency of direct and indirect BEMs, it can be proved that

$$\phi(\mathbf{s}) = [t] = t^{ext} + t^{int} \tag{10}$$

and

$$\psi(\mathbf{s}) = [u] = u^{ext} - u^{int}, \tag{11}$$

where superscript "*ext*" means the domain we treat is an infinite domain with a hole enclosed by Γ, superscript "*int*" means the domain we treat is a finite domain enclosed by Γ and [ ] means the jump of values obtained from two problems as shown in Figure 3.

Now let us give a definition of the false degeneracy of indirect BEMs by the following proposition.

Proposition. *When a non-trivial source density (single or double layer) distributes on a closed boundary Γ and it makes field quantities u and t in the interested domain, having Γ as part of its boundary, trivial at the same time, such a potential will result in a false degeneracy of the integral equation. The field quantities u and t cannot be both trivial everywhere in the counter part of the interested domain, which is equal to the free space minus the interested domain.*

This proposition is evidently true because it has been proved in reference [5] that at the true eigenvalue field quantities cannot be trivial at the same time. The reason why we introduce the indirect method is given as follows. First of all, the indirect method is more general than the direct one from mathematical point of view. In indirect methods, the distribution of a source density needs not to be on the real boundary while the direct methods require the boundary should be the real one. Another reason is that the indirect

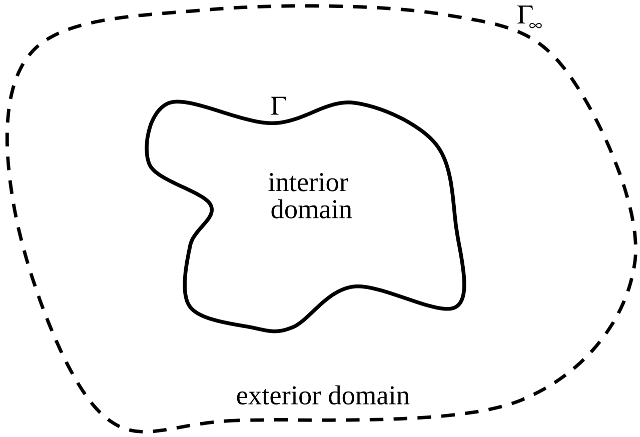

Figure 3. A closed boundary Γ, an interior domain and an exterior domain.

method actually deals with a problem with an infinite domain (free space). Therefore, we can easily explain why the false degeneracy of the integral equation for a domain occurs at the wave number that makes true degeneracy of the integral equation for its counter part, that is a domain equal to the infinite free space minus the interested domain.

3.2. NO SPURIOUS EIGENVALUES EXIST IN SOLVING THE EIGENPROBLEM OF A SIMPLY CONNECTED FINITE DOMAIN USING COMPLEX-VALUED KERNELS

Theorem 1. *For a simply connected domain, no false degeneracy exists in the single-layer potential method (double-layer potential method) using the complex-valued fundamental solution.*

Proof. For simplicity, only the single-layer potential is considered. The proof of double-layer potential method is similar to the following proof.

Now let us assume the interested simply connected domain is enclosed by the boundary Γ and there exists a non-trivial single-layer density to make u and t both trivial inside the domain. This means $u^{int} = 0$ and $t^{int} = 0$. Then from equations (10) and (8a) and continuity of u for the single-layer potential, it can be concluded that

$$\phi(\mathbf{s}) = t^{ext}(\mathbf{s}), \tag{12}$$

$$0 = \pi u^{ext}(\mathbf{x}) = \int_\Gamma U_C(\mathbf{x}, \mathbf{s}) t^{ext}(\mathbf{s})\, \mathrm{d}\Gamma(\mathbf{s}), \tag{13}$$

when $\mathbf{x}$ approaches boundary from the exterior domain. However, taking the normal derivative of equation (13), it yields

$$0 = \pi t^{ext}(\mathbf{x}) = \int_\Gamma L_C(\mathbf{x}, \mathbf{s}) t^{ext}(\mathbf{s})\, \mathrm{d}\Gamma(\mathbf{s}) = \phi(\mathbf{x}). \tag{14}$$

From equations (13) and (14), we have a physical problem for an infinite domain with a radiator having trivial boundary excitation, i.e., u and t both are trivial on the surface. It is then obvious that the solution is the trivial field, which leads to a contradiction.

Another point of view is to look at equation (12) only, it means the problem we are dealing with is an infinite domain with a radiator with boundary condition of $u = 0$. From a previous result in reference [15], the only solution is a trivial one. It leads to a contradiction; therefore, it is impossible to have a false degeneracy. □

Due to the equivalency of direct and indirect methods, one can have the following corollary.

Corollary 1. *For a simply connected domain, no false degeneracy exists in the direct singular (hypersingular) integral equation using a complex-valued fundamental solution.*

Proof. Again, only the direct singular integral equation is considered and the proof of the hypersingular integral equation is similar to that of the singular integral equation. Suppose we can obtain a false degeneracy in the direct singular integral equation using a complex-valued fundamental solution. It means that we can have a trivial field, $u = 0$ and $t = 0$, inside the domain. Then we have

$$0 = \pi u^{int}(\mathbf{s}) = RPV \int_\Gamma U_C(\mathbf{x}, \mathbf{s}) t^{int}(\mathbf{x}) \, \mathrm{d}\Gamma(\mathbf{x}) - CPV \int_\Gamma T_C(\mathbf{x}, \mathbf{s}) u^{int}(\mathbf{x}) \, \mathrm{d}\Gamma(\mathbf{x}), \quad (15)$$

when $\mathbf{s}$ approaches the boundary from the interior domain. Now let us consider its counterpart, the exterior problem, we have

$$\pi u^{ext}(\mathbf{s}) = RPV \int_\Gamma U_C(\mathbf{x}, \mathbf{s}) t^{ext}(\mathbf{x}) \, \mathrm{d}\Gamma(\mathbf{x}) - CPV \int_\Gamma T_C(\mathbf{x}, \mathbf{s}) u^{ext}(\mathbf{x}) \, \mathrm{d}\Gamma(\mathbf{x}), \quad (16)$$

when $\mathbf{s}$ approaches the boundary from the exterior domain. Assume that a non-trivial solution exists for the exterior problem with a boundary condition as $\alpha u^{ext} + \beta t^{ext} = 0$, equation (16) can be rewritten as

$$\begin{aligned} \pi u^{ext}(\mathbf{s}) &= \pi \beta \zeta(\mathbf{s}) \\ &= -\alpha \int_\Gamma U_C(\mathbf{x}, \mathbf{s}) \varsigma(\mathbf{x}) \, \mathrm{d}\Gamma(\mathbf{x}) - \beta \int_\Gamma T_C(\mathbf{x}, \mathbf{s}) \varsigma(\mathbf{x}) \, \mathrm{d}\Gamma(\mathbf{x}), \end{aligned} \quad (17)$$

where $u^{ext}(\mathbf{s}) = \beta \varsigma(\mathbf{s})$, $t^{ext}(\mathbf{s}) = -\alpha \varsigma(\mathbf{s})$ α and β cannot be both trivial at the same time.

Let us now construct its corresponding indirect integral equations from equations (8a) and (8b), we have

$$\pi u^{ext}(\mathbf{x}) = \pi \beta \varsigma(\mathbf{x}) = -\alpha \int_\Gamma \varsigma(\mathbf{s}) U_C(\mathbf{x}, \mathbf{s}) \, \mathrm{d}\Gamma(\mathbf{s}), \quad (18a)$$

$$\pi t^{ext}(\mathbf{x}) = -\pi \alpha \varsigma(\mathbf{x}) = -\alpha \int_\Gamma \varsigma(\mathbf{s}) L_C(\mathbf{x}, \mathbf{s}) \, \mathrm{d}\Gamma(\mathbf{s}). \quad (18b)$$

Comparing equation (18a) with equation (17) and by using the equality $U_C(\mathbf{x}, \mathbf{s}) = U_C(\mathbf{s}, \mathbf{x})$, we have

$$0 = \int_\Gamma \beta T_C(\mathbf{s}, \mathbf{x}) \varsigma(\mathbf{s}) \, \mathrm{d}\Gamma(\mathbf{s}) = \int_\Gamma \beta L_C(\mathbf{x}, \mathbf{s}) \varsigma(\mathbf{s}) \, \mathrm{d}\Gamma(\mathbf{s}) \quad (19)$$

by using the equality that $T_C(\mathbf{s}, \mathbf{x}) = L_C(\mathbf{x}, \mathbf{s})$. Equation (19) holds if $\beta = 0$, however, that means the exterior problem we are dealing with is a problem with $u^{ext} = 0$ which is already proved to have a trivial solution only as mentioned earlier. It leads to a contradiction thus

β cannot be zero. It then can be concluded that $\int_\Gamma L_C(\mathbf{x},\mathbf{s})\varsigma(\mathbf{s})\,\mathrm{d}\Gamma(\mathbf{s}) = 0$, then substituting it into equation (18b), we have $t^{ext} = 0$ which immediately leads to $u^{ext} = 0$ on the boundary. It leads to a contradiction too. □

3.3. SPURIOUS EIGENVALUES EXIST IN THE REAL-PART BEM

It has been found earlier that when the real-part kernels are used instead of complex kernels to solve the eigenproblem for a simply connected domain, spurious eigenvalues exist in the direct real-part BEM. Yeih *et al.* [12] have explained this phenomenon as the lack of information from the imaginary part of kernel functions. We will explain this meaning more deeply in the following. Let us begin with an indirect method using a single-layer potential. To take the real-part kernels in equations (8a) and (8b), we have the following formulations:

$$\pi u(\mathbf{x}) = \int_\Gamma U_R(\mathbf{x},\mathbf{s})\phi(\mathbf{s})\,\mathrm{d}\Gamma(\mathbf{s}), \tag{20a}$$

$$\pi t(\mathbf{x}) = \int_\Gamma L_R(\mathbf{x},\mathbf{s})\phi(\mathbf{s})\,\mathrm{d}\Gamma(\mathbf{s}), \tag{20b}$$

when $\mathbf{x}$ is in the interior domain only. Remember that equations (8a) and (8b) are valid for any $\mathbf{x}$ in a free space, it is quite different from equations (20a) and (20b). It is meaningless to let $\mathbf{x}$ be in the exterior domain in equations (20a) and (20b). For the exterior domain, equations (8a) and (8b) should be written as

$$\pi u(\mathbf{x}) = \int_\Gamma U_C(\mathbf{x},\mathbf{s})\phi(\mathbf{s})\,\mathrm{d}\Gamma(\mathbf{s}) + \lim_{\|\mathbf{s}\|\to\infty}\left[\int_{\Gamma_\infty} U_C(\mathbf{x},\mathbf{s})t(\mathbf{s})\,\mathrm{d}\Gamma(\mathbf{s}) - \int_{\Gamma_\infty} T_C(\mathbf{x},\mathbf{s})u(\mathbf{s})\,\mathrm{d}\Gamma(\mathbf{s})\right], \tag{21a}$$

$$\pi t(\mathbf{x}) = \int_\Gamma L_C(\mathbf{x},\mathbf{s})\phi(\mathbf{s})\,\mathrm{d}\Gamma(\mathbf{s}) + \lim_{\|\mathbf{s}\|\to\infty}\left[\int_{\Gamma\infty} L_C(\mathbf{x},\mathbf{s})t(\mathbf{s})\,\mathrm{d}\Gamma(\mathbf{s}) - \int_{\Gamma\infty} M_C(\mathbf{x},\mathbf{s})u(\mathbf{s})\,\mathrm{d}\Gamma(\mathbf{s})\right], \tag{21b}$$

where Γ_∞ is the boundary at infinity. The integrals at infinity approach to zero since the physical fields, u and t, satisfy the radiation condition at infinity and the complex-valued kernel functions also satisfy the radiation condition. If we take the real-parts of kernels in equations (21a) and (21b) and hope trivial quantity for integrals at infinity, it means we have a "false" boundary condition for the physical quantities, u and t, as

$$\lim_{\mathbf{s}\to\infty}\int_{\Gamma\infty} \|\mathbf{s}\|[U_R(\mathbf{x},\mathbf{s})t(\mathbf{s}) - T_R(\mathbf{x},\mathbf{s})u(\mathbf{s})]\,\mathrm{d}\phi^* = 0, \tag{22}$$

where ϕ^* represents the relative angle of $\mathbf{s}$ vector and a unit vector in x-axis.

It leads to

$$\lim_{\mathbf{s}\to\infty}\int_{\Gamma\infty} \|\mathbf{s}\|[\mathrm{Y}_0(k\sqrt{\|\mathbf{s}-\mathbf{x}\|})t(\mathbf{s}) - \mathrm{Y}_0'(k\sqrt{\|\mathbf{s}-\mathbf{x}\|})u(\mathbf{s})]\,\mathrm{d}\phi^* = 0. \tag{23}$$

Finally, by using the asymptotic expansion we can have

$$\lim_{\mathbf{s}\to\infty}\int_{\Gamma_\infty}\sqrt{||\mathbf{s}||}\Big[\cos\Big(k\sqrt{||\mathbf{s}-\mathbf{x}||}-\frac{\pi}{4}\Big)t(\mathbf{s})-\sin\Big(k\sqrt{||\mathbf{s}-\mathbf{x}||}-\frac{\pi}{4}\Big)u(\mathbf{s})\Big]\,\mathrm{d}\phi^*=0. \tag{24}$$

This condition is not a type of radiation condition, but it is then possible to have a non-trivial field for this exterior domain. By doing so, it then makes an irrational degeneracy for integral equations modelling an interior domain. The false degeneracy of integral equations for analyzing a simply connected finite domain using real-part formulations (direct or indirect) then can be understood as a wrongly posed problem by a misinterpretation of the radiation condition. In the following, we will prove that when we use the real-part BEM to deal with an eigenproblem of a simply connected domain, the non-trivial field quantity for the exterior domain should not have a projection on the Bessel functions of first kind.

If the source point, **s**, is located at a circle with radius R (R tends to infinity) and the collocation point, **x**, is located at a circle with radius $\bar{r}$, we can use equation (6) to rewrite equation (23) as

$$\begin{aligned}&\lim_{\mathbf{s}\to\infty}\int_{\Gamma\infty}||\mathbf{s}||\Big[\mathrm{Y}_0(k\sqrt{||\mathbf{s}-\mathbf{x}||})t(\mathbf{s})-\mathrm{Y}_0'(k\sqrt{||\mathbf{s}-\mathbf{x}||})u(\mathbf{s})\Big]\,\mathrm{d}\phi^*\\&=\lim_{R\to\infty}\int_{\Gamma\infty}R\left(\sum_{m=-\infty}^{\infty}\mathrm{Y}_m(kR)\mathrm{J}_m(k\bar{r})\cos(m\theta)t(\mathbf{s})-\sum_{m=-\infty}^{\infty}\mathrm{Y}_m'(kR)\mathrm{J}_m(k\bar{r})\cos(m\theta)u(\mathbf{s})\right)\mathrm{d}\phi*,\end{aligned} \tag{25}$$

where θ is the relative angle between **s** vector and **x** vector and is of course a function of ϕ^*.

The solution of u can be assumed to have a form of a linear combination of $\mathrm{J}_m(kr)\cos(m\phi^*)$, $\mathrm{J}_m(kr)\sin(m\phi^*)$, $\mathrm{Y}_m(kr)\cos(m\phi^*)$ and $\mathrm{Y}_m(kr)\sin(m\phi^*)$. If we choose a Bessel function of first kind as a basis, said $\mathrm{J}_p(kr)\cos(p\phi^*)$, then we substitute it into equation (25) and further integrate it at the circle with radius R, we can conclude that this integral cannot vanish since the following equality holds:

$$\lim_{R\to\infty}(\mathrm{Y}_m'(kR)\mathrm{J}_m(kR)-\mathrm{Y}_m(kR)\mathrm{J}_m'(kR))=\frac{c*}{R}, \tag{26}$$

where c^* is a non-zero constant.

If we choose $\mathrm{Y}_p(kr)\cos(p\phi^*)$ or $\mathrm{Y}_p(kr)\sin(p\phi^*)$ as basis functions, it perfectly makes the integral, equation (25), vanish. When p is not equal to m, the integral vanishes by the orthogonal property of triangular functions. When p is equal to m, we have

$$\lim_{R\to\infty}(\mathrm{Y}_m'(kR)\mathrm{Y}_m(kR)-\mathrm{Y}_m(kR)\mathrm{Y}_m'(kR))=0. \tag{27}$$

Therefore, we can say that the spurious eigensolution using the real-part BEM must be represented by a linear combination of $\mathrm{Y}_m(kr)\cos(m\phi^*)$ and $\mathrm{Y}_m(kr)\sin(m\phi^*)$. The coefficients of these basis functions depend on which integral formulation you use. For the singular integral formulation or single-layer potential formulation, we require a Dirichlet boundary condition, $u^{ext}=0$, on boundary Γ. On the other hand, we require a Neumann boundary condition, $t^{ext}=0$, on the boundary Γ for a hypersingular formulation or a double-layer formulation.

3.4. FICTITIOUS EIGENVALUES EXIST FOR THE EXTERIOR UNBOUNDED DOMAIN

After understanding the false degeneracy of integral equations for a simply connected finite domain, now let us consider an unbounded domain. It means we will examine the fictitious eigenvalue in various formulations.

Theorem 2. *For an unbounded domain with a radiator having a boundary Γ, the false degeneracy occurs when the complex-valued, single-layer (double-layer) potential boundary integral equation is used. The false characteristic wave numbers are the characteristic wave numbers for the free vibration problem of the radiator prescribing the Dirichlet (Neumann) boundary condition, $u = 0$ $(t = 0)$.*

Proof. Now we are looking for a non-trivial single-layer potential such that it makes a trivial field outside the radiator and correspondingly a non-trivial field inside the radiator. We need to prove the existence of such a single-layer potential, then to see what characteristics it has. From our argument, we will have $u^{ext} = 0$ and $t^{ext} = 0$ on the boundary Γ. Then from the continuity of u in the single-layer potential approach, one can have $u^{int} = 0$. It then leads to a problem of solving the eigenproblem of an interior domain (radiator) with the Dirichlet boundary condition. At the characteristic wave number for this specified eigenproblem, it then results in an irrational degeneracy for the integral equation concerning the exterior unbounded domain. □

Furthermore, we can take a look at the following corollary for the direct BEM.

Corollary 2. *For an unbounded domain with a radiator having a boundary Γ, the false degeneracy occurs when the complex-valued, direct, singular (hypersingular) boundary integral equation is used. The false characteristic wave numbers are the characteristic wave numbers for the free vibration problem of the radiator prescribing Dirichlet (Neumann) boundary condition, $u = 0 (t = 0)$.*

It is not difficult to prove Corollary 2 by the same technique used in the proof of Corollary 1. The only difference is that the interested domain now is the unbounded domain, thus its counter part is a finite domain. Therefore, a key question is can one find non-trivial boundary field quantities for the corresponding interior problem. The answer is for sure positive because all finite domains may have a natural resonance once non-dissipative boundary conditions are prescribed on the boundary. As usual, the type of boundary condition relates to a single-layer potential approach or a direct, singular integral equation is the Dirichlet type. On the other hand, the Neumann type boundary condition relates to a double-layer approach or a direct, hypersingular integral equation.

3.5. PSEUDO-FICTITIOUS EIGENVALUES EXIST FOR A MULTIPLY CONNECTED FINITE DOMAIN

We have examined a simply connected domain and an unbounded domain with a radiator. To continue our exploration, we will take a look at a multiply connected domain.

Theorem 3. *For a multiply connected domain shown in Figure 4 and the indirect, complex-valued, single-layer (double-layer) potential boundary integral equation is used, the false degeneracy, i.e., pseudo-fictitious eigensolution, depends on the eigenproblem of the inner hole prescribing the Dirichlet (Neumann) condition.*

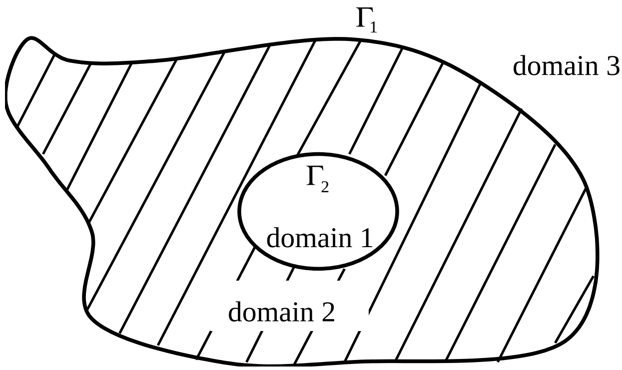

Figure 4. A multiply connected domain.

Proof. Let us first divide the whole space into three regions: the inner region (domain 1), the interested domain (domain 2) and the exterior unbounded region (domain 3). We then denote the field quantities, **u** and **t**, on the boundary with subscripts 1, 2 and 3, respectively, to specify the domains currently being dealt with. From the above argument, we can say that now we are looking for a non-trivial distribution of ϕ on boundaries Γ_1 and Γ_2 such that $\mathbf{u_2} = \mathbf{0}$ and $\mathbf{t_2} = \mathbf{0}$ on Γ_1 and Γ_2. For domain 3, since $\mathbf{u_3} = \mathbf{0}$ on Γ_1 (continuity of **u**) it can be concluded that $\mathbf{t_3} = \mathbf{0}$ on Γ_1 physically. For domain 1, since $\mathbf{u_1} = \mathbf{0}$ on Γ_1 continuity of **u**), the non-trivial $\mathbf{t_1}$ on boundary Γ_1 can be found at the characteristic wave number for the Dirichlet problem of the domain 1. It then completes the proof. □

A simple view of this proof is that for a multiply connected domain, the counter part of an interested domain has two parts, domain 1 and domain 3. For domain 2, our interested domain, domain 1 is an interior domain and domain 3 is an exterior domain. To seek the possibility of the false degeneracy when modelling a domain with a boundary integral equation is equivalent to seek a "physically" possible rank deficiency for its counter part. Since domain 1 is interior to domain 2, the characteristic wave number of domain 1 makes irrational degeneracy of integral equation for domain 2. Again, the type of these irrational characteristic wave numbers depends on which integral equation one uses.

Finally, we will have the following corollary for the direct method by the equivalency of the direct and indirect methods.

Corollary 3. *For a multiply connected domain shown in Figure 4 and the direct, complex-valued, singular (hypersingular) boundary integral equation is used, the false degeneracy, i.e., pseudo-fictitious eigensolution, depends on the eigenproblem of the inner hole prescribing the Dirichlet (Neumann) condition.*

There are some interesting remarks worth mentioning here. First for all, if one let Γ_1 extend to infinity, the false degeneracy (pseudo-fictitious eigensolution) then becomes the well-known fictitious eigenvalue [16, 17]. Our proof reconfirms the results obtained in Chen's work [18]. However, our proof is much more general as compared with Chen's proof.

Furthermore, it is wondered what will happen for a multiply connected finite region using a real-part BEM. It can be quickly concluded that another type of non-trivial potential on boundary Γ_1 becomes possible, and the corresponding false eigenequation

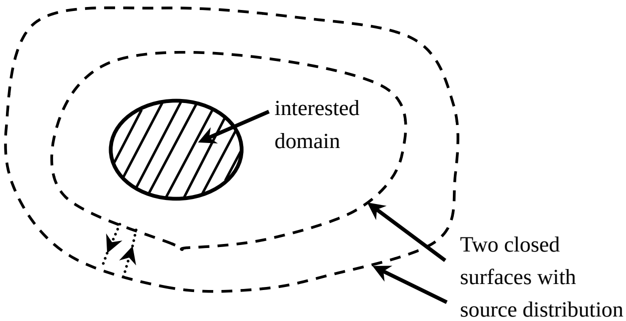

Figure 5. A distribution of sources on a multiply connected type boundary results in the false degeneracy when solving the eigneproblem of a simply connected domain.

(spurious eigenequation) depends on the shape of Γ_1 and the type of integral equations one uses.

3.6. SOME REMARKS

Application of the general theory mentioned here can yield many interesting results. For example, when we use the complex-valued single-layer potential to solve an eigenproblem of a simply connected finite domain, it is possible to have degeneracy of integral equations once we allow the potential distributes not only on a simple closed boundary. As shown in Figure 5, we can arrange our single-layer potential on two closed curves. Then from our argument, we can quickly conclude that the degeneracy of integral equations occurs at a characteristic wave number of the corresponding Dirichlet problem of a multiply connected domain enclosed by two curves where the single-layer potential distributes on. Other application on the half-plane problem has been worked out and will be submitted soon.

Before closing this section, we would like to give some comments here. The fictitious eigenvalue (handling the radiation or scattering problem for an unbounded exterior domain using the complex-valued formulation), the spurious eigenvalue (handling a free vibration problem of a finite domain using the real-part BEM formulation) and the pseudo-fictitious eigenvalue (handling a multiply connected finite domain using real-part or complex-valued BEM formulation) are basically the same. Mathematically speaking, they all encounter the rank deficiency problem in an indefinite form of 0/0. Furthermore, finding such a rank deficiency is equivalent to a problem of finding a potential distribution such that all the field quantities become trivial in the interested domain and non-trivial field quantities exist in the counter part.

4. NUMERICAL EXAMPLES

In the following examples, we will validate our arguments mentioned in previous sections. Let us begin with a circular membrane with radius equal to 1 and subjected to the Dirichlet boundary condition. Using different direct BEMs will result in different spurious eigenequations and these results are shown in Table 1. This case is a benchmark problem mentioned in the earlier research. Now let us find what will happen when one solve this simple problem by introducing a domain partition scheme.

Example 1. The unit circle domain is partitioned into two semi-circles.

In this example, it is impossible for us to derive eigenvalues, true or false, analytically. The purposes we design this numerical example are: first, we will verify that when a domain is partitioned into several simply connected domains, pseudo-fictitious eigenvalues will not appear as predicted in the previous section; second, by comparing the result of this example with that of the next one, it will be concluded that the positions where the false degeneracy occurs depend on the partitioning scheme.

In Figure 6, the complex-valued UT method is used to solve this problem. The singular-value decomposition method is adopted to check the degeneracy of the influencing matrix. It can be seen that in this partitioning scheme no false degeneracy occurs in the complex-valued UT method. In this figure and following ones, the analytical values of degenerated wave numbers are marked in the bracket once they are available.

Figure 7 illustrates the results obtained from the real-part UT method. Comparing these results with those in Figure 6, it is easy to find that the real-part formulation results in some unwanted rank deficiencies. Since these unwanted rank deficiencies do not appear in the complex-valued BEM, it can be concluded that they are spurious eigenvalues.

Before closing this example, we combine the real-part UT and LM equations together to construct an over-determined system as mentioned in section 2. As shown in Figure 8, it can be found that this method successfully filters out spurious eigenvalues resulting from the real-part formulation. It should be mentioned here that such a technique is not superior to using the complex-valued UT or LM equation alone. When we combine the real-part UT and LM equations together, it means that we have as many equations as we have in the complex-valued UT or LM equation. It then becomes meaningless to adopt the real-part formulation in the very beginning. However, using real-part formulations will save computation effort in a problem involving a multiply connected domain as mentioned in the following examples.

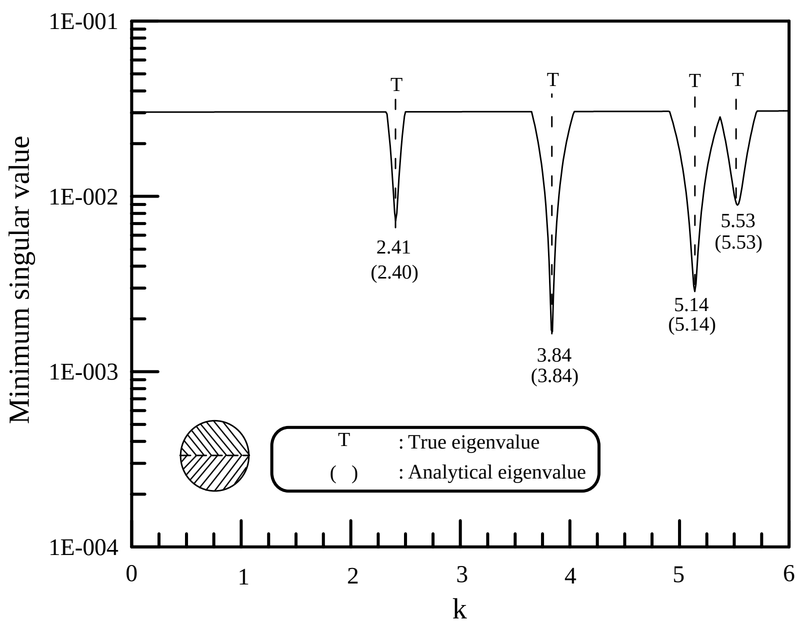

Figure 6. Solving a Dirichlet problem of a unit circle using the complex-valued UT equation and partitioning the domain into two semi-circles.

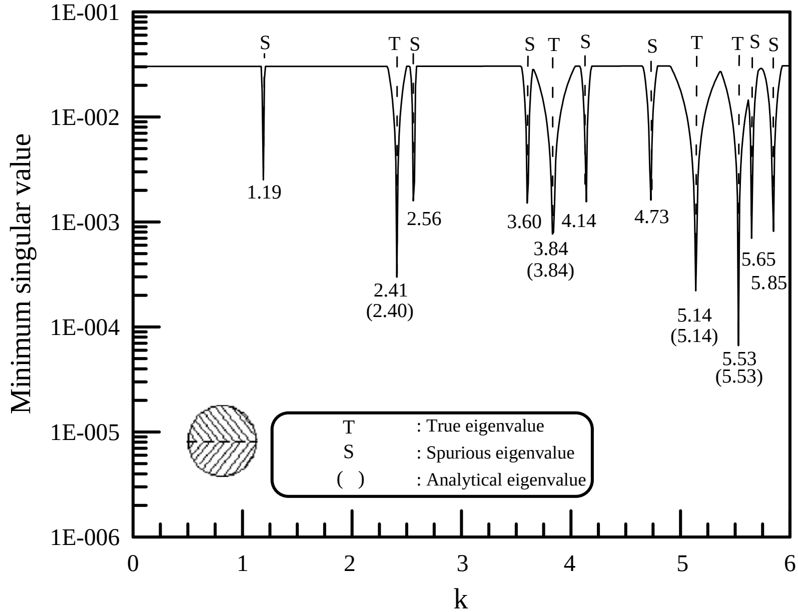

Figure 7. Solving a Dirichlet problem of a unit circle using the real-part UT equation and partitioning the domain into two semi-circles.

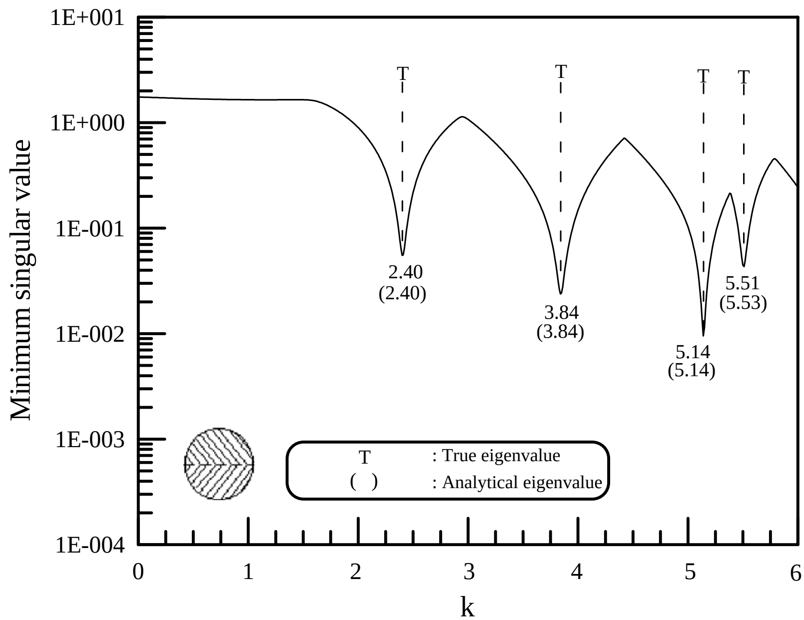

Figure 8. Filtering out spurious eigensolutions by a combined use of real-part UT and LM equations.

Example 2. The unit circle now is divided into two regions, one is simply connected and the other is multiply connected. The simply connected one is a circular domain with a radius $r_2 = 0{\cdot}5$ and the multiply connected domain is an annular region with an outer radius $r_1 = 1{\cdot}0$ and an inner radius $r_2 = 0{\cdot}5$.

In this example, a multiply connected domain is included in the domain partitioning. As predicted from the previous section, the pseudo-fictitious type of degeneracy should appear even in a complex-valued formulation. From Figures 9 and 10, we can find that some unwanted rank deficiencies appear in this partitioning scheme no matter where the complex-valued UT or LM formulation is used. We call this kind of rank deficiency as the pseudo-fictitious eigenvalue.

Besides the pseudo-fictitious eigenvalues, the real-part formulation suffers another kind of false degeneracy, the spurious eigenvalues. The above-mentioned results using the real-part UT equation are shown in Figure 11.

Comparing these results obtained in this example with those in the previous one, it can further be found that the false rank deficiencies appear in different wave numbers when the partitioning scheme is changed. In our previous research [9], we have already pointed this out. This method can be considered as another alternative to filter out the false rank deficiencies. However, additional mesh is required and it becomes not economical in numerical practice.

In the previous example, we have mentioned that a combined use of the real-part UT and LM equations together does not save computation effort in the numerical sense. However, in this example using real-part formulations is superior to using complex-valued UT or/and LM equations. This is because of a multiply connected domain existing in the partitioning scheme. When a multiply connected domain exists, even the complex-valued UT or LM equation will result in false degeneracy. Therefore, using real-part UT and LM equations together to construct an over-determined system indeed saves computation effort as compared with using complex-valued formulations. In Figure 12, we can filter out

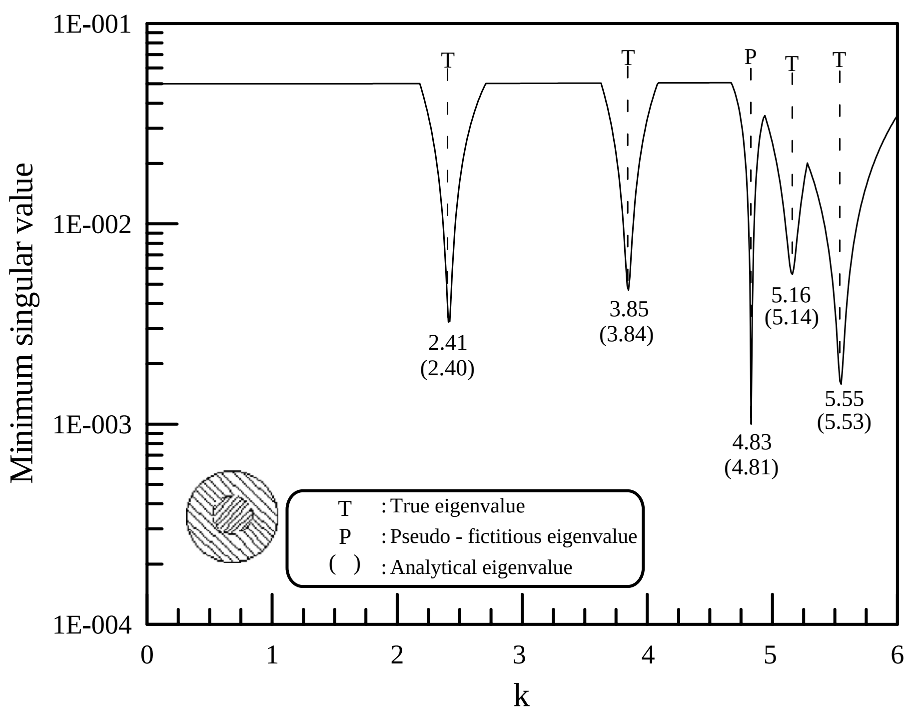

Figure 9. Pseudo-fictitious eigenvalues appear in solving a Dirichlet problem of a unit circle using the complex-valued UT equation and partitioning the unit circle into two subdomains: a circle and an annular region.

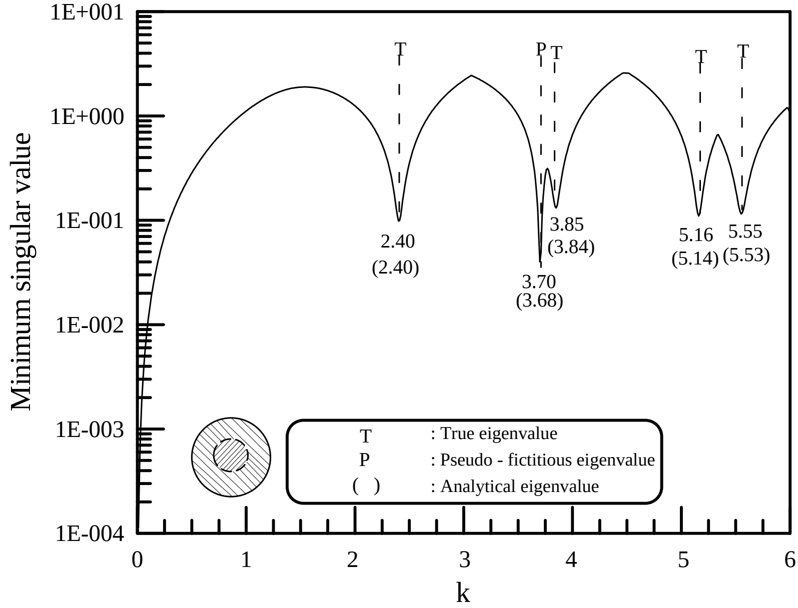

Figure 10. Pseudo-fictitious eigenvalues appear in solving a Dirichlet problem of a unit circle using the complex-valued LM equation and partitioning the unit circle into two subdomains: a circle and an annular region.

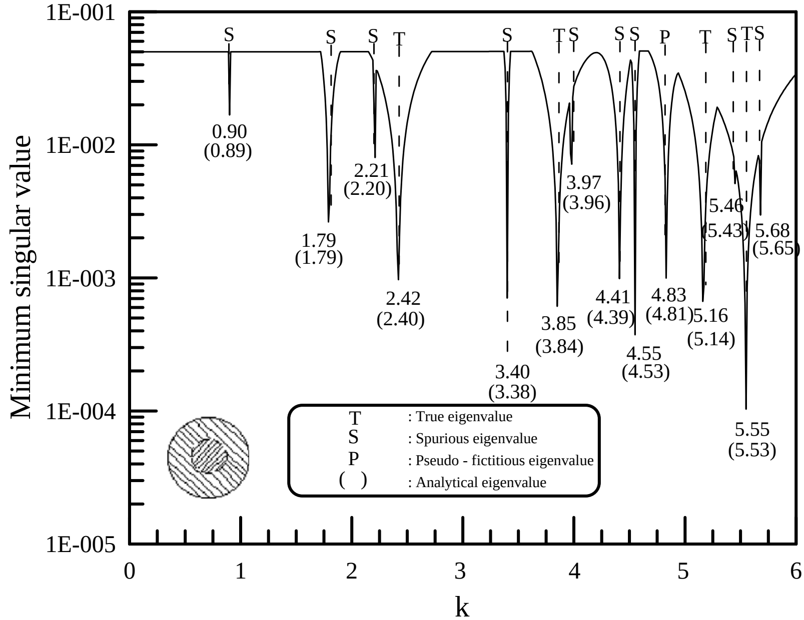

Figure 11. Both spurious and pseudo-fictitious eigenvalues appear in solving a Dirichlet problem of a unit circle using the real-part UT equation and partitioning the unit circle into two subdomains: a circle and an annular region.

all kinds of false rank deficiencies by combining the real-part UT and LM equations together.

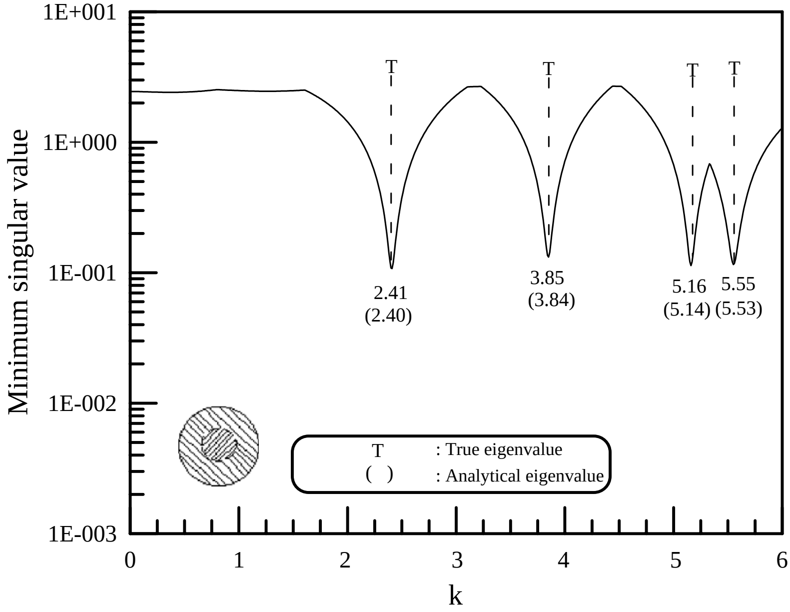

Figure 12. Eliminating spurious and pseudo-fictitious eigenvalues by a combined use of the real-part UT and LM equations.

Example 3. An annular region with an outer radius equal to 1.0 and an inner radius equal to 0.5 is considered.

In the previous example, the pseudo-fictitious eigenvalues are found. We have illustrated in the previous example that this kind of false degeneracy occurs due to the existence of a multiply connected domain. Now, let us solely look at this multiply connected domain.

First, let us prescribe the Dirichlet boundary condition on the boundary and use the complex-valued UT method. As seen in Figure 13, the positions where pseudo-fictitious eigenvalues occur are very close to the results in Figure 9. It then confirms our argument that a multiply connected domain results in pseudo-fictitious rank deficiencies.

To eliminate the false degeneracy, we have proposed two alternatives in section 2. Demonstrations for using singular and hypersingular equations together have been shown, now let us take a look at another alternative. The second method to filter out the false degeneracy is to perform an operation on the 0/0 indefinite form by the generalized singular-value decomposition method. As mentioned in reference [5], the false rank deficiencies occur simultaneously in the original problem and its auxiliary problem, whose boundary condition is homogeneous, linearly independent of the original problem. For a Dirichlet problem, one can use the Neumann problem as its auxiliary problem. The real-part UT equation is adopted here. In Figure 14(a), we have rank deficiencies of the original problem. In Figure 14(b), we have rank deficiencies of $\begin{bmatrix} U_R^T \\ T_R^T \end{bmatrix}$ The common eigenvalues in both graphs are false ones as proved in reference [5].

We further claim that the pseudo-fictitious or spurious eigenvlaues are independent of boundary conditions. Now let us take a look at the Neumann problem. We here adopt the real-part UT equation to analyze the eigenproblem. As shown in Figure 15, we can find out that both the pseudo-fictitious or spurious eigenvalues are very close to the results of the Dirichlet problem as shown in Figure 14(a).

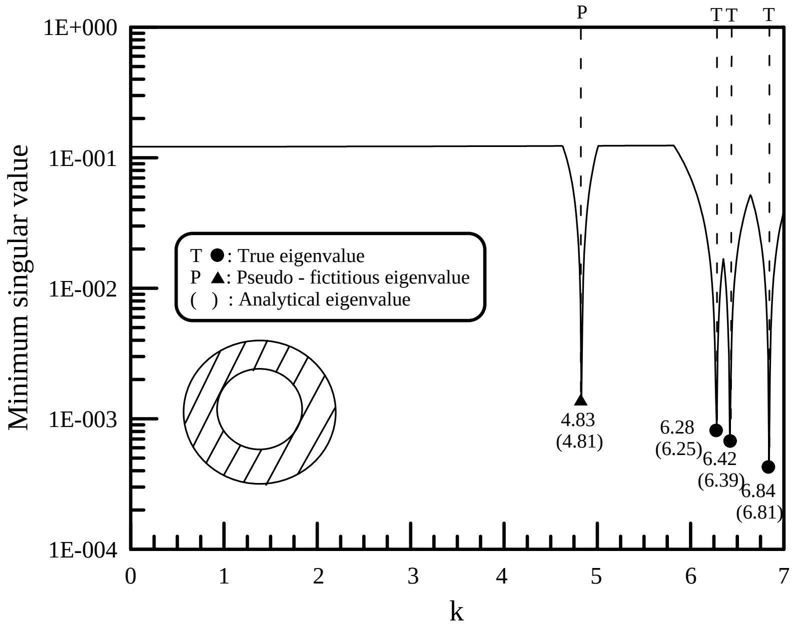

Figure 13. Solving the Dirichlet problem of an annular region by the complex-valued UT equation.

Example 4. A square region with edge length equal to 2 is divided into two regions. The first region is a circular domain located at the center of the square with radius equal 0·5. The second region is a multiply connected domain, which is simply a square region with a circular hole. The Dirichlet boundary condition is given in this case.

As we mentioned in the previous section, the pseudo-fictitious eigenvalues only depend on the type of integral equations we used and the geometry of the hole in a multiply connected domain. The first part of the above description has been demonstrated numerically, we now use this numerical example to demonstrate the second part. Comparing the geometry in this example with that in Example 2, we can find that the same part is the hole of the multiply connected domain, which is a circular region with radius 0·5. Since we only concern with the pseudo-fictitious eigenvalue, we can adopt the complex-valued UT or LM equation. The result for complex-valued UT method is shown in Figure 16. The analytical values for true eigenvalues can be found in reference [11]. Comparing Figure 16 with Figure 9, we can confirm that when the type of integral equations is chosen and the geometries of inner holes in the multiply connected subdomains are the same, pseudo-fictitious eigenvalues occur at the same wave numbers for both of the problems.

Example 5. In this example, a circular domain with an eccentric square hole is considered as shown in Figure 17. A Dirichlet boundary condition is given on the boundary.

The reason we design this example is to reconfirm that the pseudo-fictitious eigenvalue depends on the geometry of the inner hole of a multiply connected domain but has nothing to do with the position where it is located. In previous examples, one may argue that some kinds of symmetry can be found. However, no symmetry property exists in this case.

We here use Kuo's approach [5] to look at the false degeneracy. Since only the pseudo-fictitious eigenvalue is concerned, we simply use the complex-valued UT equation for demonstration. After performing the QR factorization of $\begin{bmatrix} U_C^{\mathrm{T}} \\ T_C^{\mathrm{T}} \end{bmatrix}$ system, the rank deficiency

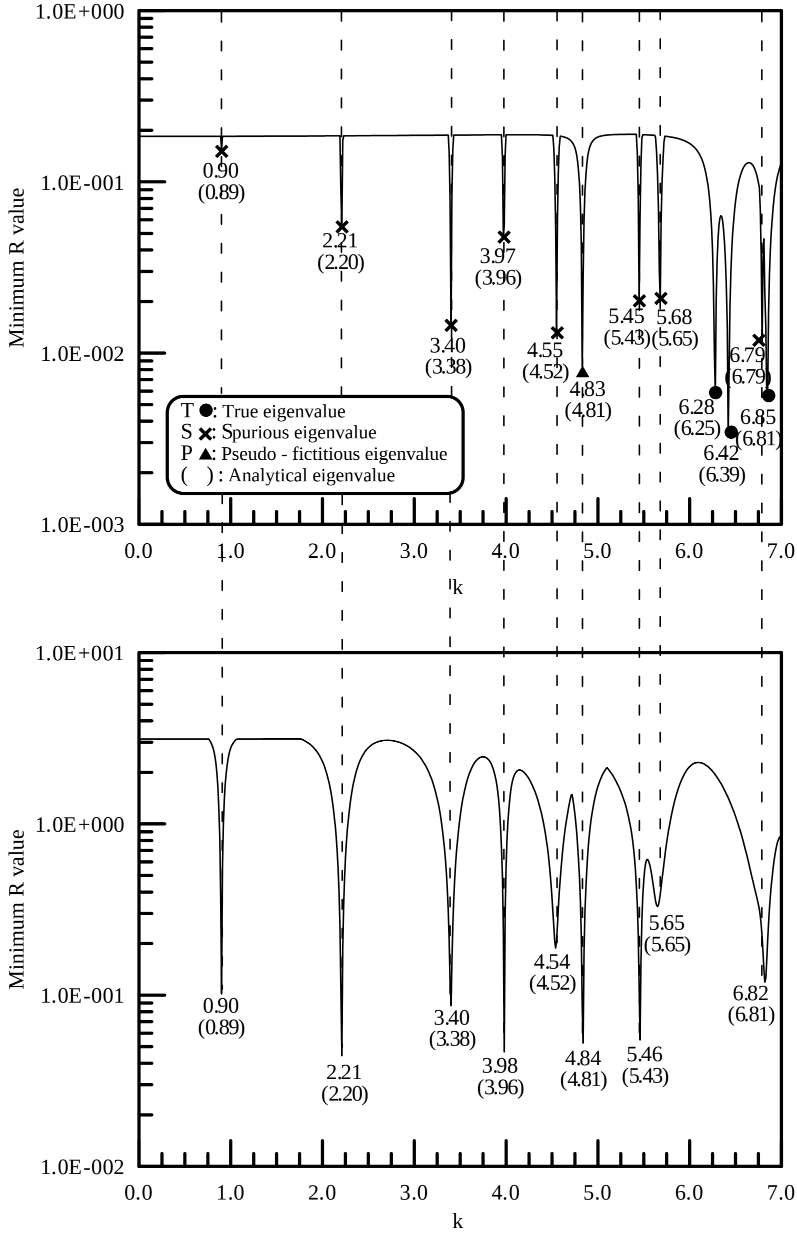

Figure 14. Eliminating the false degeneracy in solving a Dirichlet problem of an annular region using the real-part UT equation by comparing the degeneracy of two problems: (a) the original problem, both the true and false rank deficiencies exist; (b) the common part in the original problem and its auxiliary problem, only false rank deficiency exists.

occurring in **R** matrix is the false degeneracy. It can be found in Figure 18 that all numerically computed pseudo-fictitious eigenvalues match analytical predictions very well.

Before we close this section, we show the numerical results of true eigenmodes in Example 4. The first three eigenmodes for a square domain are shown in Figure 19(a)–(c).

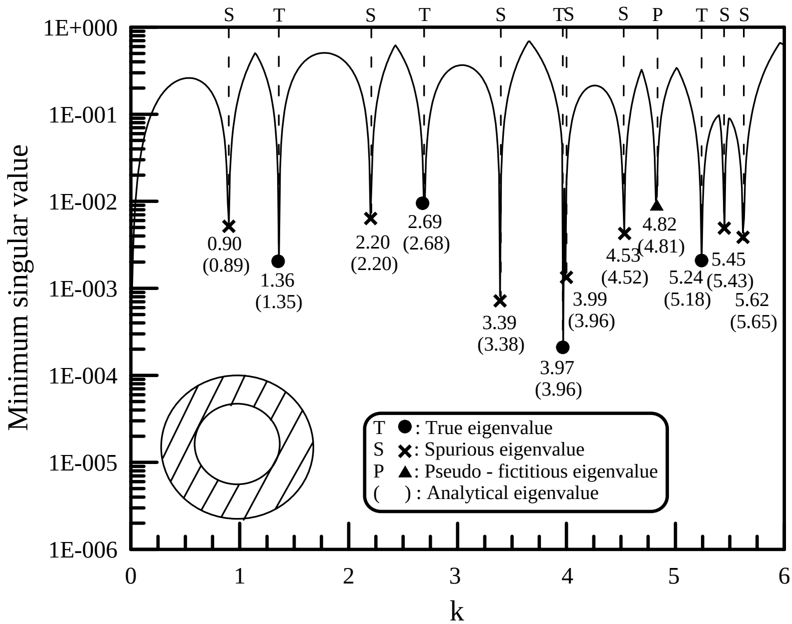

Figure 15. Solving the Neumann problem of an annular region by the real-part UT equation.

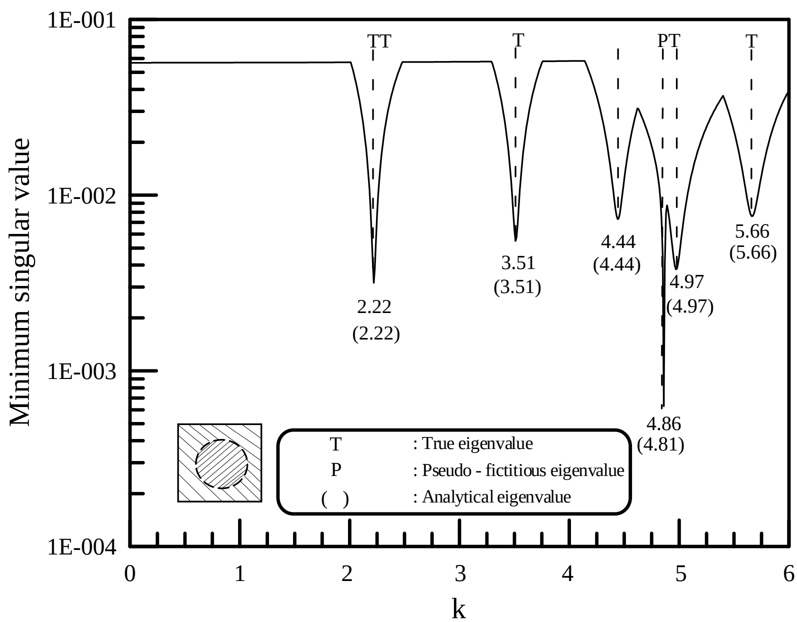

Figure 16. Solving a Dirichelt problem of the square region using the complex-valued UT equation and partitioning the domain into two subdomains and one of them is a multiply connected domain.

The dotted lines in these figures are the artificial interface in the domain partitioning. It should be mentioned here that we compute these eigenmodes in every subdomain independently by first obtaining those eigendata on the real boundary and interface.

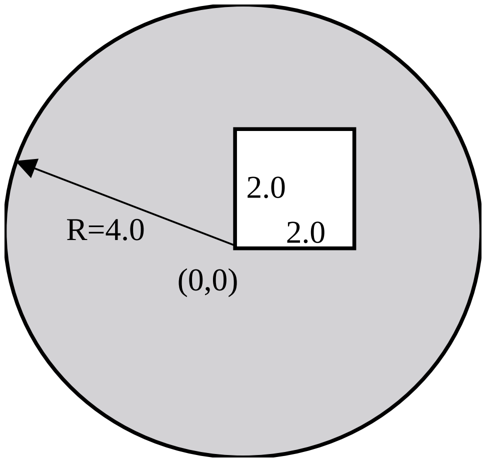

Figure 17. A multiply connected domain: a circular domain with an eccentric square hole.

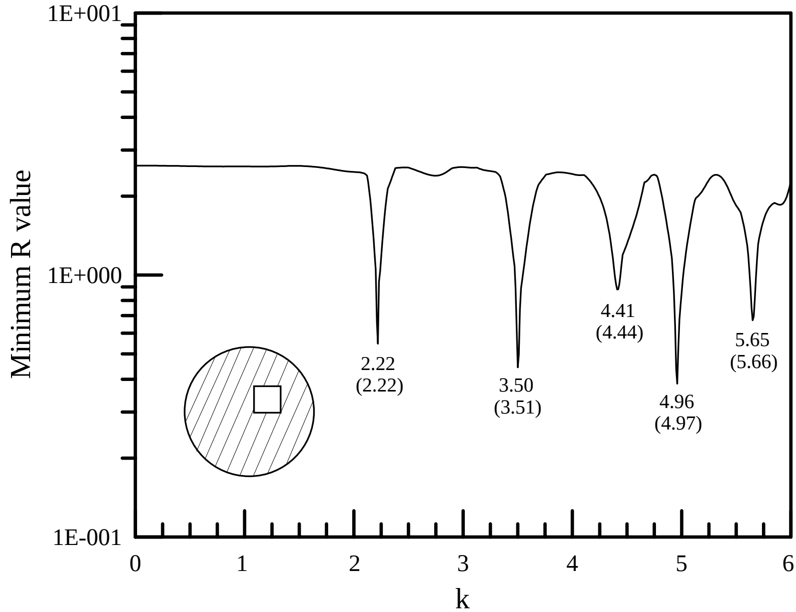

Figure 18. The pseudo-fictitious eigenvalue depends on the geometry of inner hole.

5. CONCLUSIONS

In this paper, a new type of spurious eigenvalues arising due to the multiply connected domain has been discovered and further validated both by the numerical and analytical calculations. We have proposed a new point of view for the false degeneracy of the Helmholtz boundary integral equations to unify the spurious eigenvalue, fictitious eigenvalue and pseudo-fictitious eigenvalue. We also prove that the false degeneracy occurs when a non-trivial source distribution (single layer or double layer) exists to make the field quantities in the interested domain trivial. Such false degeneracy is independent of the boundary condition but dependent on the type of integral equations one uses.

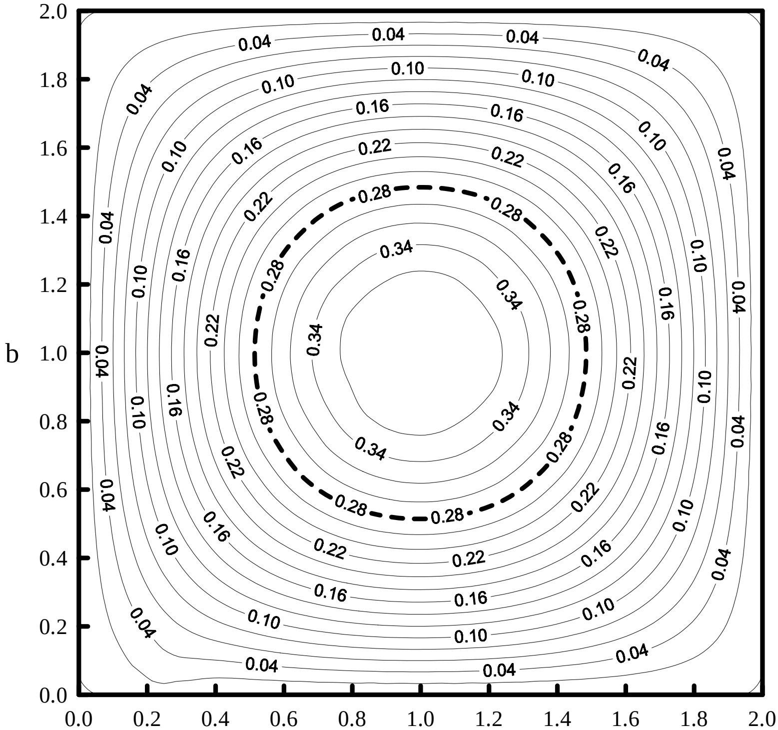

(a)

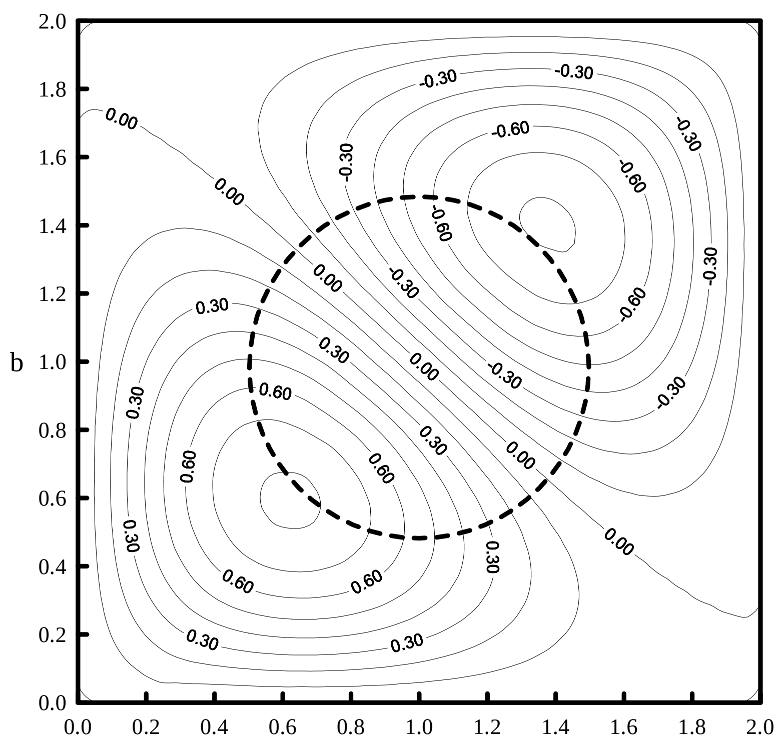

(b)

Figure 19. The first three modes of the Dirichlet case of a square domain: (a) the first mode; (b) the second mode; (c) the third mode.

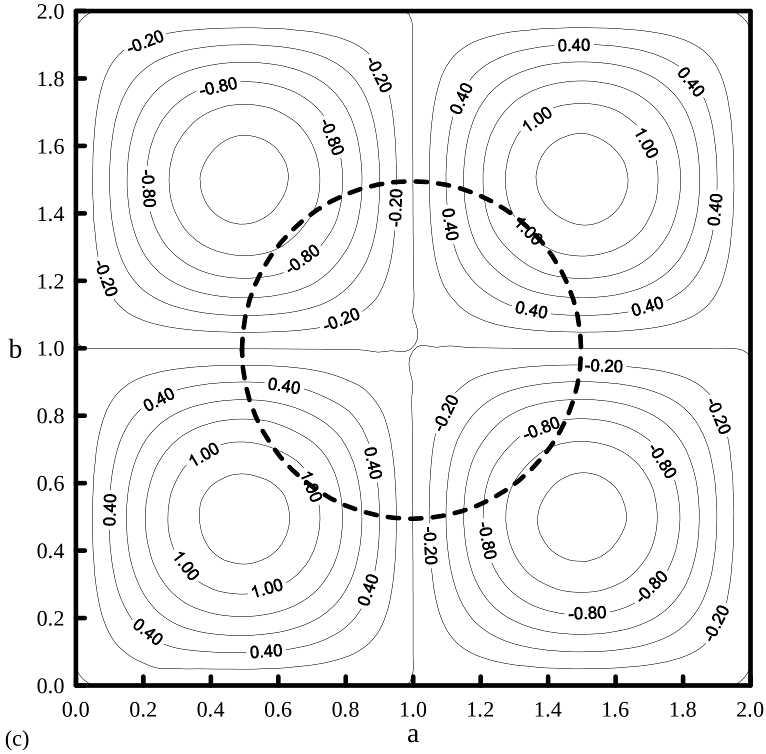

Figure 19. Continued.

Furthermore, pseudo-fictitious eigenvalues depend on the geometry of inner hole of a multiply connected domain. Numerical results match our analytical predictions very well.

REFERENCES

1. G. De Mey 1976 *International Journal for Numerical Methods in Engineering* **10**, 59–66. Calculation of the Helmholtz equation by an integral equation.
2. Y. Niwa, S. Kobayashi and M. Kitahara 1982 in *Development in Boundary Element Methods* (P. K. Banerjee and R. Shaw, editors, Vol. 2) New York: Applied Science Publisher, Chapter 7. Determination of eigenvalue by boundary element methods.
3. G. De Mey 1977 *International Journal for Numerical Methods in Engineering* **11**, 1340–1342. A simplified integral equation method for the calculation of the eigenvalues of Helmholtz equation.
4. J. R. Hutchinson 1985 in *Boundary Elements VII*, 6.13–6.25 (C. A. Brebbia and G. MAIER). Berlin: Springer-Verlag. An alternative BEM formulation applied to membrane vibrations.
5. S. R. Kuo, W. Yeih and Y. C. Wu 2000 *Journal of Sound and Vibration* **235**, 813–845. Applications of the generalized singular-value decomposition method on the eigenproblem using the incomplete boundary element formulation.
6. J. T. Chen and F. C. Wong 1997 *Engineering Analysis with Boundary Elements* **20**, 25–33. Analytical derivations for one-dimensional eigenproblems using dual BEM and MRM.
7. W. Yeih, J. T. Chen and C. M. Chang 1999 *Engineering Analysis with Boundary Elements* **23**, 339–360. Applications of dual MRM for determining the natural frequencies and natural modes of an Euler-Bernoulli beam using the singular value decomposition method.
8. W. Yeih, J. R. Chang, C. M. Chang and J. T. Chen 1999 *Advances in Engineering Software* **30**, 459–468. Application of dual BEM for determining the natural frequencies and natural modes of a rod using the singular value decomposition method.

9. J. R. Chang, W. Yeih and J. T. Chen 1999 *Computational Mechanics* **24**, 29–30. Determination of natural frequencies and natural modes of a rod using the dual BEM in conjunction with the domain partition technique.
10. J. R. Chang and W. Yeih 2001 *Journal of the Chinese Institute of Engineers* **24**, 151–171. Applications of domain partition in BEM for solving the vibration problem.
11. J. T. Chen, K. H. Chen and S. W. Chyuan 1999 *Applied Acoustics* **57**, 293–325. Numerical experiments for acoustic modes of a square cavity using the dual boundary element method.
12. W. Yeih, J. T. Chen, K. H. Chen, F. C. Wong 1998 *Advances in Engineering Software* **29**, 1–6. A study on the multiple reciprocity method and complex-valued formulation for the Helmholtz equation.
13. S. R. Kuo, J. T. Chen, C. X. Huang 2000 *International Journal for Numerical Methods in Engineering* **48**, 1401–1422. Analytical study and numerical experiments for true and spurious eigenvalues of a circular cavity using real-part BEM.
14. J. R. Chang 1999 *Ph.D. Thesis, National Taiwan Ocean University, Keelung, Taiwan, R. O. C.* Applications of Domain Partitioning on Vibration Problems using Dual BEM.
15. F. John 1950 *Communications in Pure and Applied Mathematics* **3**, 45–101. On the motion of floating bodies, II.
16. H. A. Schenck 1968 *Journal of the Acoustical Society of America* **44**, 41–58. Improved integral formulation for acoustic radiation problem.
17. A. J. Burton and G. F. Miller 1971 *Proceeding of Royal Society, London, Series A.* **323**, 201–210. The application of integral equation methods to the numerical solutions of some exterior boundary value problems.
18. J. T. Chen 1998 *Mechanics Research Communications* **23**, 529–534. On fictitious frequencies using dual series representation.